

Impact of intrinsic charm amount in the nucleon and saturation effects on the prompt atmospheric ν_μ flux for IceCube

Victor P. Goncalves,^{1,*} Rafał Maciula,^{2,†} and Antoni Szczurek^{c2,§}

¹*Instituto de Física e Matemática, Universidade Federal de Pelotas (UFPel),
Caixa Postal 354, CEP 96010-900, Pelotas, RS, Brazil*

²*Institute of Nuclear Physics, Polish Academy of Sciences,
Radzikowskiego 152, PL-31-342 Kraków, Poland*

(Dated: July 14, 2021)

Abstract

The predictions for the atmospheric neutrino flux at high energies strongly depend on the contribution of prompt neutrinos, which are determined by the production of charmed meson in the atmosphere at very forward rapidities. In this paper we estimate the related cross sections taking into account the presence of an intrinsic charm (IC) component in the proton wave function and the QCD dynamics modified by the onset of saturation effects. The impact on the predictions for the prompt neutrino flux is investigated assuming different values for the probability to find the IC in the nucleon. Comparison with the IceCube data is performed and conclusions are drawn.

arXiv:2103.05503v2 [hep-ph] 13 Jul 2021

^c also at University of Rzeszów, PL-35-959 Rzeszów, Poland

^{*} barros@ufpel.edu.br

[†] rafal.maciula@ifj.edu.pl

[§] antoni.szczurek@ifj.edu.pl

I. INTRODUCTION

The understanding of Particle Physics have been challenged and improved by the recent experimental results obtained by the LHC, the Pierre Auger and IceCube Neutrino Observatories [1]. In particular, in recent years, IceCube measured the astrophysical and atmospheric neutrinos fluxes at high energies [2–4] and different collaborations from the LHC performed several analyses of the heavy meson production at high energies and forward rapidities [5–8]. Such distinct sets of data are intrinsically related, since the description of the heavy meson production at the LHC and higher center of mass energies is fundamental to make predictions of the prompt neutrino flux [9], which is expected to dominate the atmospheric ν flux for large neutrino energies [10]. An important question, which motivate the present study, is whether the current and future IceCube data can shed light on charm production at the LHC and vice - versa and in particular on the intrinsic charm in the nucleon.

In order to derive realistic predictions of the prompt atmospheric neutrino flux at the detector level we should have theoretical control of the description of several ingredients (see Fig. 1): the incident cosmic flux, the charm production, its hadronization, the decay of the heavy hadrons, the propagation of the associated particles through the atmosphere and the neutrino interaction (see e.g. Refs. [11–19]). As demonstrated in our previous study [9], to address the production of high-energy neutrinos ($E_\nu > 10^5$ GeV), it is fundamental to precisely describe the charmed meson production at very high energies and large forward rapidities. This aspect motivated the development of new and/or more precise approaches to describe the perturbative and nonperturbative regimes of the Quantum Chromodynamics (QCD) needed to describe the charmed meson production in a kinematical range beyond that reached in hadronic collisions at the LHC. For this new kinematical range, some topics are theme of intense debate: (a) the presence (or not) of intrinsic heavy quarks in the hadronic wave function [20–22], characterized by a large value of the longitudinal momentum fraction of beam nucleon momentum; (b) the validity of the collinear factorization at high energies [23–26], since it disregards the transverse momentum of the incident particles; and (c) the presence (or not) of nonlinear (saturation) effects on the description of the QCD dynamics at high energies [27], which are expected to contribute at high energies due to the high partonic density predicted by linear DGLAP or BFKL evolution equations; (d) the impact of subleading fragmentation of light partons on heavy meson production at high energies and very forward rapidities and its consequences for prompt neutrino flux [19, 28]. Such questions naturally arise due to the fact that in the calculation of the prompt neutrino flux at high energies, the main contribution for the charm production cross section comes from partons with very small (large) values of x in the hadrons that constitute the atmosphere (incident cosmic ray flux). Recently, two of us have presented in Ref. [29] a comprehensive study of the charm production at large rapidities considering the collinear, hybrid and k_T -factorization approaches taking into account the presence of an intrinsic charm in the proton wave function with parton distributions that are solutions of linear and nonlinear evolution equations. One of the goals of this paper is to extend the analysis performed in Ref. [29] and derive associated prompt neutrino fluxes at high energies. In particular, we shall estimate the impact of the intrinsic charm – initiated subprocess and/or saturation effects on the predictions for the prompt neutrino flux. Another more ambitious goal is to verify whether the recent IceCube data for the prompt ν_μ flux allow to derive an upper bound for the probability of finding a charm quark-antiquark pair in the proton wave function, which is one of the main uncertainties in the modelling of the intrinsic charm. A similar goal was also

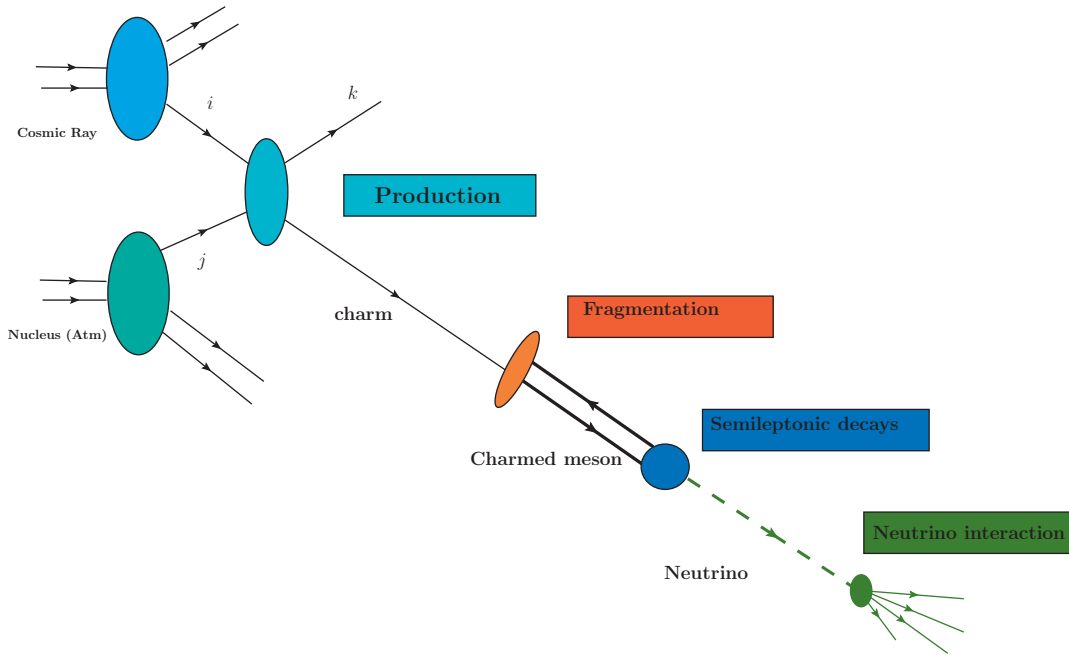


FIG. 1. Representation of the ingredients needed to estimate the prompt neutrino flux at the detector level.

present in the analyses performed in Refs. [14, 16]. However, our study differs from these previous analyses in several aspects. Our predictions for the x_F distributions will be derived using a framework that successfully describes the LHC data, with the main input being the parton distribution functions which were derived using the world data. In these previous studies, the x_F distribution was fitted using the old data for the D and Λ_c production, with the normalization being a parameter free. Moreover, the energy dependence of the intrinsic charm contribution was assumed to follow the inelastic cross section, which is dictated by soft processes. In contrast, in our approach, such contribution is calculated perturbatively, which implies a steeper energy dependence. Finally, our predictions are calculated using a unified approach for the $gg \rightarrow c\bar{c}$ and $gc \rightarrow gc$ mechanisms, which we believe to be more realistic to treat the charm production at central and forward rapidities.

The paper is organized as follows. In the next section a brief review of formalism needed to estimate the prompt ν_μ flux is presented. In particular, we discuss the Z -moment method [30], the hybrid approach for production of c/\bar{c} quarks/antiquarks and the main inputs and underlying assumptions of our calculations. In Section III, we shall present our predictions for the Feynman x_F distribution and for the prompt flux considering different charm production mechanisms and different models for the unintegrated gluon distribution. Moreover, the prompt flux is estimated assuming different amounts for the probability of finding an intrinsic charm component in the nucleon and the predictions are compared with the recent IceCube data. Finally, in Section IV we shall summarize our main results and formulate conclusions.

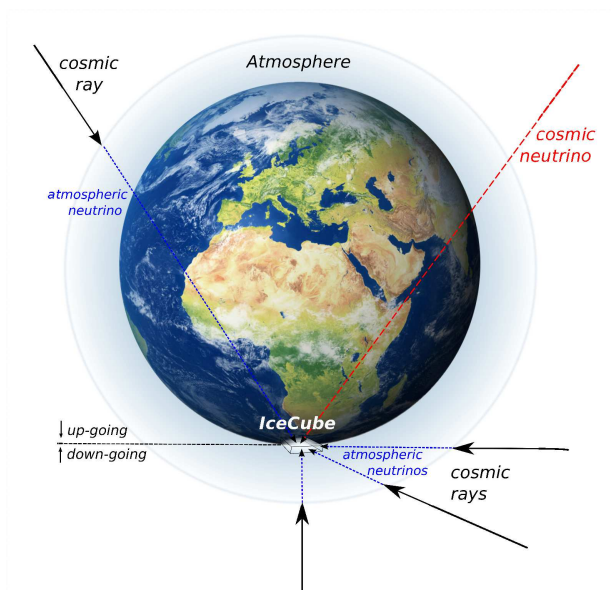


FIG. 2. A schematic illustration of the IceCube experiment.

II. FORMALISM

A schematic illustration of the IceCube experiment is shown in Fig. 2. Neutrinos are detected through the Cherenkov light emitted by secondary particles produced in neutrino-nucleon interactions in or around the detector. Although primarily designed for the detection of high-energy neutrinos from astrophysical sources, denoted cosmic neutrino in Fig. 2, IceCube can also be used for investigating the atmospheric neutrino spectrum. The atmospheric neutrinos are produced in cosmic-ray interactions with nuclei in Earth's atmosphere [10]. While at low neutrino energies ($E_\nu \lesssim 10^5$ GeV), these neutrinos arise from the decay of light mesons (pions and kaons), and the associated flux is denoted as the *conventional* atmospheric neutrino flux [32], for larger energies it is expected that the *prompt* atmospheric neutrino flux associated with the decay of hadrons containing heavy flavours become important [30]. One has that the flux of conventional atmospheric neutrinos is a function of the zenith angle, since horizontally travelling mesons have a much higher probability to decay before losing energy in collisions, which implies a harder conventional neutrino spectrum of horizontal events compared to vertical events. In contrast, heavy mesons decay before interacting and follow the initial spectrum of cosmic rays more closely, being almost independent of the zenith angle in the neutrino energy range probed by the IceCube. As discussed in the Introduction, the calculation of the prompt atmospheric neutrino flux at the detector level depends on the description of the production and decay of the heavy hadrons as well as the propagation of the associated particles through the atmosphere (see Fig. 1). Following our previous studies [9, 19], we will estimate the expected prompt neutrino flux in the detector ϕ_ν using the Z -moment method [30], which implies that ϕ_ν can be estimated using the geometric interpolation formula

$$\phi_\nu = \sum_H \frac{\phi_\nu^{H,low} \cdot \phi_\nu^{H,high}}{\phi_\nu^{H,low} + \phi_\nu^{H,high}}. \quad (1)$$

where $H = D^0, D^+, D_s^+$, Λ_c for charmed hadrons and $\phi_\nu^{H,low}$ and $\phi_\nu^{H,high}$ are solutions of a set of coupled cascade equations for the nucleons, heavy mesons and leptons (and their antiparticles) fluxes in the low- and high-energy ranges, respectively. They can be expressed in terms of the nucleon-to-hadron (Z_{NH}), nucleon-to-nucleon (Z_{NN}), hadron-to-hadron (Z_{HH}) and hadron-to-neutrino ($Z_{H\nu}$) Z -moments, as follows [30]

$$\phi_\nu^{H,low} = \frac{Z_{NH}(E) Z_{H\nu}(E)}{1 - Z_{NN}(E)} \phi_N(E, 0), \quad (2)$$

$$\phi_\nu^{H,high} = \frac{Z_{NH}(E) Z_{H\nu}(E)}{1 - Z_{NN}(E)} \frac{\ln(\Lambda_H/\Lambda_N)}{1 - \Lambda_N/\Lambda_H} \frac{m_H c h_0}{E \tau_H} f(\theta) \phi_N(E, 0), \quad (3)$$

where $\phi_N(E, 0)$ is the primary flux of nucleons in the atmosphere, m_H is the decaying particle's mass, τ_H is the proper lifetime of the hadron, $h_0 = 6.4$ km, $f(\theta) \approx 1/\cos\theta$ for $\theta < 60^\circ$, and the effective interaction lengths Λ_i are given by $\Lambda_i = \lambda_i/(1 - Z_{ii})$, with λ_i being the associated interaction length ($i = N, H$). For $Z_{H\nu}$, our treatment of the semileptonic decay of D -hadrons follows closely Ref. [15]. In particular, we assume the analytical decay distributions $H \rightarrow \mu\nu_\mu X$ obtained in Ref. [31] and use the decay branching ratios reported in the most recent PDG [1]. For a detailed discussion of the cascade equations, see e.g. Refs. [11, 30]. Assuming that the incident flux can be represented by protons ($N = p$), the charmed hadron Z -moments are given by

$$Z_{pH}(E) = \int_0^1 \frac{dx_F}{x_F} \frac{\phi_p(E/x_F)}{\phi_p(E)} \frac{1}{\sigma_{pA}(E)} \frac{d\sigma_{pA \rightarrow H}(E/x_F)}{dx_F}, \quad (4)$$

where E is the energy of the produced particle (charmed meson), x_F is the Feynman variable, σ_{pA} is the inelastic proton-Air cross section and $d\sigma/dx_F$ is the differential cross section for the charmed meson production. Following previous studies [11–19], we will assume that $A = 14$, i.e. we will take the ^{14}N nucleus as the most representative element in the composition of the atmosphere. For this value of the atomic mass number, it is a reasonable approximation to assume that $\sigma_{pA \rightarrow charm} \approx A \times \sigma_{pp \rightarrow charm}$. Surely a more refine analysis of these two aspects is possible but would shadow our discussion of the selected issues. For σ_{pA} we will assume the prediction presented in Ref. [33] (for a more detailed discussion see Ref. [34]).

The transition from quarks to hadrons in our calculations is done within the independent parton fragmentation picture (see e.g. Ref. [47]). It is done assuming that the hadron pseudorapidity is equal to parton pseudorapidity and only momenta of hadrons are reduced compared to the parent partons. In such an approximation the charmed meson x_F -distributions at large x_F can be obtained from the charm quark/antiquark x_F^c -distributions as:

$$\frac{d\sigma_{pp \rightarrow H}(x_F)}{dx_F} = \int_{x_F}^1 \frac{dz}{z} \frac{d\sigma_{pp \rightarrow charm}(x_F^c)}{dx_F^c} D_{c \rightarrow H}(z), \quad (5)$$

where $x_F^c = x_F/z$ and $D_{c \rightarrow H}(z)$ is the relevant fragmentation function (FF). Here, in the numerical calculations we take the traditional Peterson FF [48] with $\varepsilon = 0.05$. The resulting meson distributions are further normalized by the proper fragmentation probabilities.

As discussed in Ref. [29], the cross section for the charm production at large forward rapidities, which is the region of interest for estimating the prompt ν_μ flux [9], can be expressed as follows

$$d\sigma_{pp \rightarrow charm} = d\sigma_{pp \rightarrow charm}(gg \rightarrow c\bar{c}) + d\sigma_{pp \rightarrow charm}(cg \rightarrow cg), \quad (6)$$

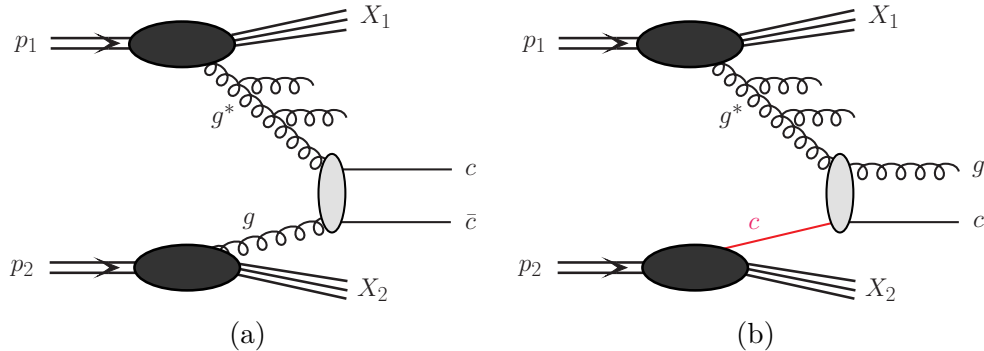


FIG. 3. A sketch of the (a) $gg^* \rightarrow c\bar{c}$ and (b) $cg^* \rightarrow cg$ production mechanisms in pp -interactions within the hybrid model.

where the first and second terms represent the contributions associated with the $gg \rightarrow c\bar{c}$ and $cg \rightarrow cg$ mechanisms, with the corresponding expressions depending on the factorization scheme assumed in the calculations. In Ref. [29], a detailed comparison between the collinear, hybrid and k_T -factorization approaches was performed. In what follows, we will focus on the hybrid factorization model, which is based on the studies performed also in Refs. [23–26]. Such a choice is motivated by: (a) the theoretical expectation that the collinear approach, largely used in previous calculations of ϕ_ν , breaks down at very small- x [24, 26]; and that (b) the k_T -factorization approach reduces to the hybrid model in the dilute-dense regime, which is the case in the charm production at very forward rapidities, where we are probing large (small) values of x in the projectile (target). In this approach, the differential cross sections for $gg^* \rightarrow c\bar{c}$ and $cg^* \rightarrow cg$ mechanisms, sketched in Fig. 3, are given by

$$d\sigma_{pp \rightarrow charm}(gg \rightarrow c\bar{c}) = \int dx_1 \int \frac{dx_2}{x_2} \int d^2k_t g(x_1, \mu^2) \mathcal{F}_{g^*}(x_2, k_t^2, \mu^2) d\hat{\sigma}_{gg^* \rightarrow c\bar{c}} \quad (7)$$

and

$$d\sigma_{pp \rightarrow charm}(cg \rightarrow cg) = \int dx_1 \int \frac{dx_2}{x_2} \int d^2k_t c(x_1, \mu^2) \mathcal{F}_{g^*}(x_2, k_t^2, \mu^2) d\hat{\sigma}_{cg^* \rightarrow cg}, \quad (8)$$

where $g(x_1, \mu^2)$ and $c(x_1, \mu^2)$ are the collinear PDFs in the projectile, $\mathcal{F}_{g^*}(x_2, k_t^2, \mu^2)$ is the unintegrated gluon distribution (gluon uPDF) of the proton target, μ^2 is the factorization scale of the hard process and the subprocesses cross sections are calculated assuming that the small- x gluon is off mass shell and are obtained from a gauge invariant tree-level off-shell amplitude. In our calculations $c(x_1, \mu^2)$, similarly $\bar{c}(x_1, \mu^2)$, contain the intrinsic charm component.

As emphasized in Ref. [29], the hybrid model, already at leading-order, takes into account radiative higher-order corrections associated with extra hard emissions that are resummed by the gluon uPDF. In the numerical calculations below the intrinsic charm PDFs are taken at the initial scale $m_c = 1.3$ GeV, so the perturbative charm contribution is intentionally not taken into account when discussing IC contributions.

Considering the $cg^* \rightarrow cg$ mechanism one has to deal with the massless partons (minijets) in the final state. The relevant formalism with massive partons is not yet available. Therefore it is necessary to regularize the cross section that has a singularity in the $p_t \rightarrow 0$ limit. We follow here the known prescription adopted in PYTHIA, where a special suppression factor

is introduced at the cross section level. The form factor depends on a free parameter p_{t0} , which will be fixed here using experimental data for the D meson production in $p + p$ and $p + {}^4\text{He}$ collisions at $\sqrt{s} = 38.7$ GeV and 86 GeV, respectively.

The predictions for the charm production strongly depend on the modelling of the partonic content of the proton [29]. In particular, the contribution of the charm - initiated process is directly associated with the description of the extrinsic and intrinsic components of the charm content in the proton (for a recent review see, e.g. Ref. [35]). Differently from the extrinsic charm quarks/antiquarks that are generated perturbatively by gluon splitting, the intrinsic one have multiple connections to the valence quarks of the proton and thus is sensitive to its nonperturbative structure [20–22]. The presence of an intrinsic component implies a large enhancement of the charm distribution at large x (> 0.1) in comparison to the extrinsic charm prediction. Moreover, due to the momentum sum rule, the gluon distribution is also modified by the inclusion of intrinsic charm. In recent years, the presence of an intrinsic charm (IC) component have been included in the initial conditions of the global parton analysis [36, 37], the resulting IC distributions that are compatible with the world experimental data. However, its existence is still a subject of intense debate [38, 39], mainly associated with the amount of intrinsic charm in the proton wave function, which is directly related to the magnitude of the probability to find an intrinsic charm or anticharm (P_{ic}) in the nucleon.

In our analysis we will consider the collinear PDFs given by the CT14nnloIC parametrization [37] from a global analysis assuming that the x -dependence of the intrinsic charm component is described by the BHPS model [20]. In this model the proton light cone wave function has higher Fock states, one of them being $|qqq\bar{c}\bar{c}\rangle$. The cross sections will be initially estimated in the next section using the set obtained for $P_{ic} = 1\%$ and, for comparison, the results for the case without IC will also be presented. Another important ingredient is the modelling of $\mathcal{F}_{g^*}(x_2, k_t^2, \mu^2)$, which depends on the treatment of the QCD dynamics for the unintegrated gluon distribution at small- x . Currently, there are several models in the literature, some of them have been reviewed in Ref. [29]. In our analysis we shall consider three different models: two based on the solutions of linear evolution equations, which disregard nonlinear (saturation effects) and one being the solution of the Balitsky-Kovchegov equation [40], which takes into account these effects in the small- x regime. In particular, we will use the uPDF derived using the Kimber-Martin-Ryskin (KMR) prescription [41], which assumes that the transverse momentum of the partons along the evolution ladder is strongly ordered up to the final evolution step. In the last step this assumption breaks down and the incoming parton that enters into the hard interaction posses a large transverse momentum ($k_t \approx \mu$). Such prescription allow us to express $\mathcal{F}_{g^*}(x_2, k_t^2, \mu^2)$ in terms of Sudakov form factor, which resums all the virtual contributions from the scale k_t to the scale μ , and a collinear g PDF, which satisfies the DGLAP evolution equations. For this model, we will estimate the uPDF using as input the CT14nnlo parametrization (with and without IC) [37] and the associated predictions will be denoted as KMR hereafter. Some time ago we showed that in the case of charm production at the LHC, the KMR uPDF leads to a reasonable description of the experimental data for D -meson and $D\bar{D}$ -pair production [42]. As also discussed in Refs. [43, 44], the KMR model effectively includes extra emission of hard partons (gluons) from the uPDF that corresponds to higher-order contributions and leads therefore to results well consistent with collinear NLO approach. In order to investigate the impact of new dynamical effects – beyond those included in the DGLAP equation – that are expected to be present in the small- x regime, we will also estimate the charm cross section

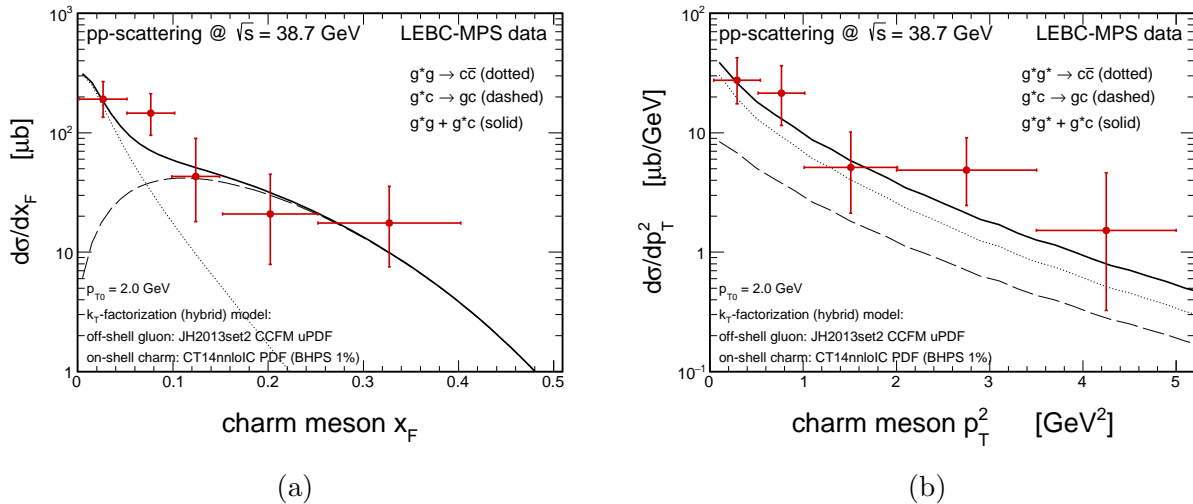


FIG. 4. Predictions of the hybrid model for (a) the Feynman x_F - and (b) the transverse momentum distributions of charm particles produced in pp collisions at $\sqrt{s} = 39$ GeV. Presented here data are from Ref. [50].

using as input the uPDF's obtained in Ref. [45] as a solution of the Balitsky-Kovchegov equation [40] modified to include the sub-leading corrections in $\ln(1/x)$ which are given by a kinematical constraint, DGLAP P_{gg} splitting function and the running of the strong coupling (for a detailed derivation see Ref. [46]). Such an approach includes the corrections associated with the BFKL equation, in an unified way with the DGLAP one, as well the nonlinear term, which takes into account unitarity corrections. In Ref. [45] the authors performed a fit to the combined HERA data and provided the solutions with and without the inclusion of the nonlinear term. In the next section, we will use these solutions as input in our calculations and the corresponding predictions will be denoted KS nonlinear and KS linear, respectively. For a comparison between predictions for the KMR, KS linear and KS nonlinear $\mathcal{F}_{g^*}(x_2, k_t^2, \mu^2)$ we refer the interested reader to Fig. 7 in Ref. [29].

III. RESULTS

In what follows we will present our predictions for the prompt atmospheric neutrino flux derived using the Z -moment method. The effective hadronic interaction lengths Λ_i and the Z_{pp} , Z_{HH} and $Z_{H\nu}$ -moments will be estimated following Ref. [12]. On the other hand, the Z_{pH} -moment will be calculated using as input the x_F -distribution for the charm production derived in the hybrid approach with the ingredients discussed in the previous section. Moreover, the prompt ν_μ flux will be evaluated considering the description of the primary spectrum proposed by Gaisser in Ref. [49], denoted as H3a spectrum, which assumes that it is given by a composition of 3 populations and 5 representative nuclei, with the set of parameters determined by a global fit of the cosmic ray data.

As discussed in the previous Section, the predictions for the $cg \rightarrow cg$ mechanism are calculated assuming that the partons in the final state are massless, which implies introduction of a cutoff p_{t0} to regularize the singularity in the partonic cross section (see [29]). In order

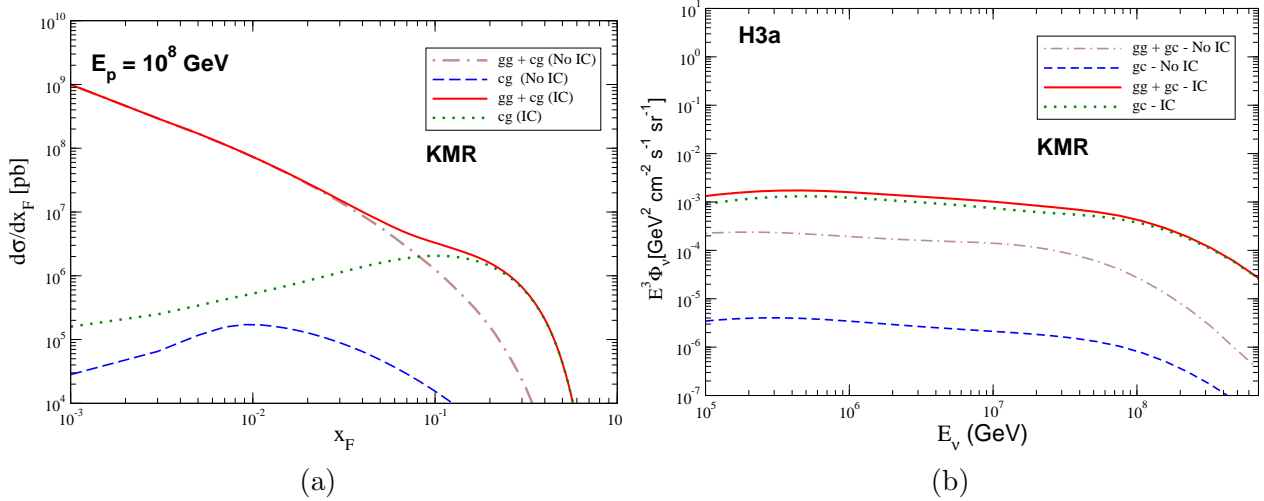


FIG. 5. Predictions of the hybrid model for (a) the Feynman x_F - distributions for charm particles and (b) the prompt neutrino flux (rescaled by E_ν^3), calculated using the KMR model for the uPDF. The predictions with and without the presence of an intrinsic charm (here $p_{t0} = 2$ GeV was used) are presented separately. The H3a parametrization of the cosmic ray flux is used in this calculation.

to constrain this parameter, we will initially consider the LEBC - MPC data [50] for the D meson production in pp collisions at $\sqrt{s} = 39$ GeV. In Fig. 4 we present our predictions for the x_F and p_T distributions of the charm meson, obtained using the CT14nnloIC parametrization for $P_{ic} = 1\%$ in the calculation of the $cg \rightarrow cg$ mechanism. The results for the x_F distribution indicate that the inclusion of the $cg^* \rightarrow cg$ mechanism is needed in order to describe the data. Moreover, the p_T distribution is also well described. Both results point out that a value of $p_{t0} = 2.0$ GeV is a good choice for the cutoff, which can be considered conservative, since smaller values imply a larger amount for the contribution of the $cg \rightarrow cg$ mechanism. Such choice is also justified by the recent analysis performed in Ref. [51], where a comprehensive study of the impact of an intrinsic charm component on the D meson production in pHe fixed - target collisions at the LHCb was performed. The results presented in Ref. [51] indicate that the LHCb data can be well described assuming $p_{t0} = 2.0$ GeV for a probability of 1% of finding a charm quark-antiquark pair in the proton wave function.

In Fig. 5 (a), we present our predictions for the Feynman x_F distribution of charm particles produced in pp collisions at the atmosphere, considering an incident proton with an energy of $E_p = 10^8$ GeV and the KMR model for the uPDF. Similar conclusions are derived using the KS linear and KS nonlinear uPDFs. We present separately the contribution associated with the $cg \rightarrow cg$ mechanism and the sum of the two mechanisms, denoted by “cg” and “gg + cg”, respectively. Moreover, we compare the IC predictions, obtained using the CT14nnloIC parametrization for $P_{ic} = 1\%$, with those obtained disregarding the presence of the intrinsic component (denoted No IC hereafter). One has that for small $x_F (\equiv x_1 - x_2)$, the charm production is dominated by the $gg \rightarrow c\bar{c}$ mechanism, which is expected since for $x_F \approx 0$ and high energies both longitudinal momentum fractions x_i are very small and the proton structure is dominated by gluons. For the No IC case, the contribution of the $cg \rightarrow cg$ mechanism is smaller than the gluon fusion one for all values of x_F . In contrast, when intrinsic charm is included, the behavior of the distribution in the intermediate x_F

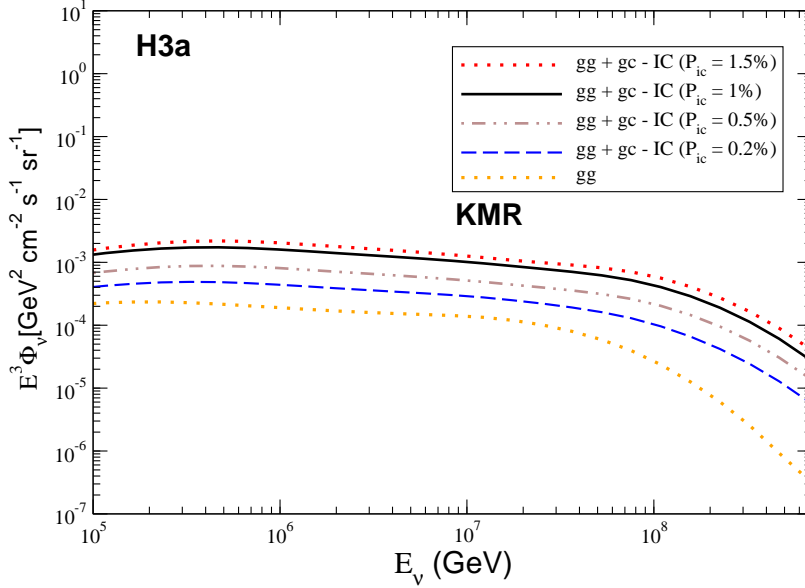


FIG. 6. Predictions of the hybrid model for the prompt neutrino flux (rescaled by E_ν^3), calculated using the KMR model for the uPDF. The IC contribution was obtained with $p_{t0} = 2$ GeV and assuming different values for the probability to find an intrinsic charm. The H3a parametrization of the cosmic ray flux is used in this calculation.

range ($0.06 \leq x_F \leq 0.6$) is strongly modified. Such a behaviour is expected, since for this kinematical range, the charm production depends on the description of the partonic content of the incident proton at large values of the Bjorken x variable. As discussed in the previous section, the main impact of the presence of an intrinsic charm is that the charm distribution is enhanced at large x (> 0.1), becoming larger than the gluon distribution. As a consequence, the presence of an intrinsic charm implies that the Feynman x_F -distribution for large x_F is dominated by the $cg \rightarrow cg$ mechanism. The impact on the predictions for the prompt neutrino flux is presented in Fig. 5 (b). As expected from the analysis performed in Ref. [9], where we find that the dominant contribution to the neutrino flux comes typically from x_F in the region $0.2 < x_F < 0.5$, one has that the flux is enhanced by one order of magnitude when intrinsic charm is present. In agreement with the results presented in Fig. 5 (a), the contribution of the $cg \rightarrow cg$ mechanism is negligible for the No IC case. However, it becomes dominant in the IC case, with the normalization of the prompt flux dependent on the amount of IC present in the projectile proton, as demonstrated in Fig. 6, where we compare the prediction derived assuming $P_{ic} = 1\%$, which is the assumption present in the CT14nloIC parametrization, with the results obtained assuming different values for this probability in the calculation of the x_F distribution for the $cg \rightarrow cg$ mechanism. As expected from Eqs. (1), (4) and (8), our results indicate that ϕ_ν is linearly dependent on P_{ic} and, therefore, a precise determination of the prompt neutrino flux can be used, in principle, to constrain the amount of IC in the proton (see below).

The charm production at large x_F is also dependent on the small- x content of the target proton, which is dominated by gluons. The dependence of our results on the model assumed to describe the unintegrated gluon distribution is analyzed in Fig. 7, where we present the predictions for the x_F distribution and for the prompt neutrino flux derived assuming the

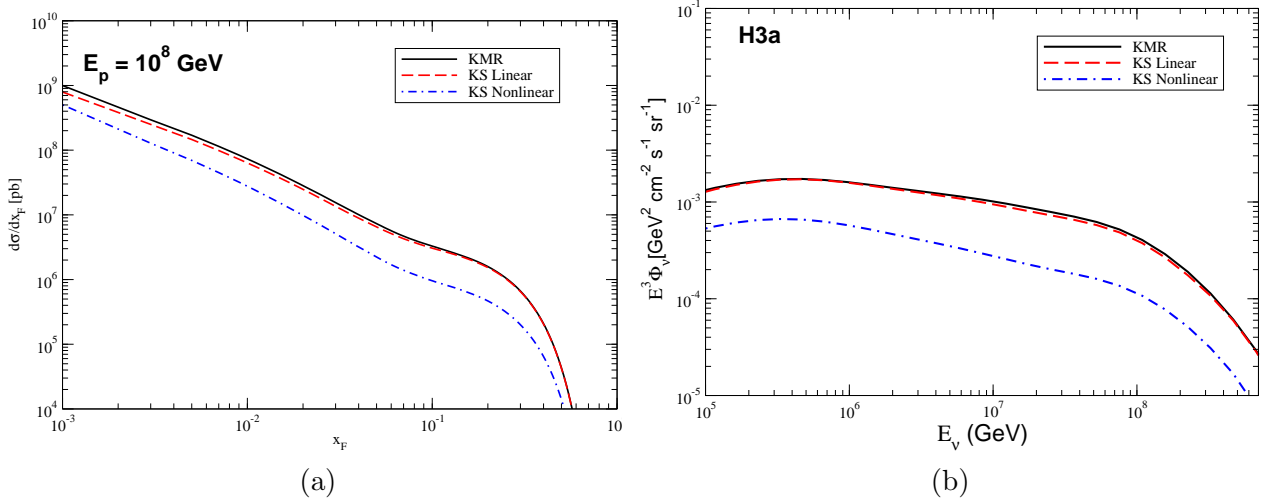


FIG. 7. Predictions of the hybrid model for the (a) Feynman x_F - distributions for charm particles and (b) the prompt neutrino flux (rescaled by E_ν^3), derived assuming different models for the uPDF. The H3a parametrization of the cosmic ray flux is used in this calculation.

KMR, KS linear and KS nonlinear models as input in our calculations. For this analysis, we only present the sum of the two mechanisms for charm production and the IC predictions. One has that KMR and KS linear predictions for the x_F distribution are similar, with the KMR one being slightly larger for small x_F . On the other hand, the KS nonlinear is a factor ≈ 3 smaller for $x_F = 0.2$. Such a result demonstrates that the inclusion of the BFKL effects in modelling \mathcal{F}_{g^*} has a small effect on the behaviour of the distribution for large x_F . In contrast, the inclusion of the nonlinear (saturation) effects strongly modifies the magnitude of the distribution. A similar conclusion is derived from the analysis of Fig. 7(b), where we present our predictions for the prompt neutrino flux. One important aspect is that the saturation effects imply a suppression of the flux in the kinematical range probed by the IceCube ($E_\nu \lesssim 10^7$ GeV).

Our results indicate that the presence of the intrinsic charm implies enhancement of the prompt ν_μ flux, while the saturation effects suppress it for high energies. Another important aspect is that the impact of the $cg \rightarrow cg$ mechanism depends on the magnitude of P_{ic} . One important question is whether the current or future experimental IceCube data can be used to probe the presence of these effects and constrain the probability to find an IC on the proton structure, i.e. whether those data could help to improve our understanding of the strong interactions theory. In recent years the IceCube Collaboration measured the energy spectrum of atmospheric neutrino flux with larger precision in an extended energy range [2, 3] and more data are expected in the forthcoming years [52, 53]. Such measurements are a challenge due to steeper falling behaviour expected for the atmospheric flux in comparison to that associated with astrophysical neutrinos. Different methods have been proposed to disentangle these two contributions with promising results (see e.g. Ref. [52]). Therefore, the posed question is valid, relevant and timely.

The IceCube apparatus can measure directions of neutrinos/antineutrinos [10]. The IceCube experimental data discussed below is selected taking into account only such ν_μ neutrinos that passed through the Earth (see Fig. 2). In Fig. 8 we present our results for the atmospheric ν_μ flux, scaled by a factor E_ν^2 , which is the sum of the conventional and prompt

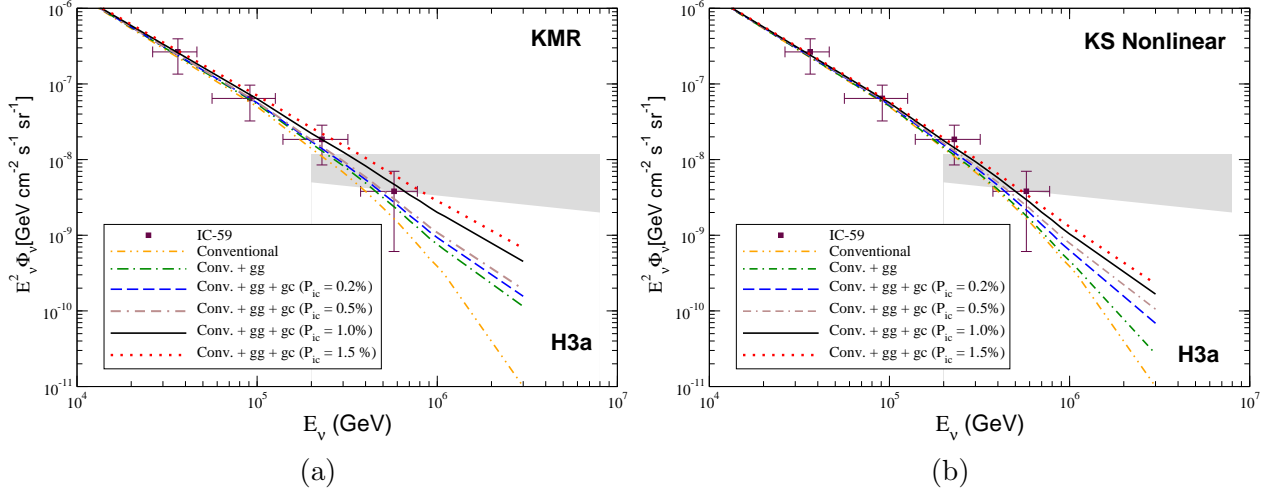


FIG. 8. Comparison between our predictions and the experimental IceCube data [2] for the atmospheric ν_μ flux for (a) KMR and (b) KS nonlinear uPDFs. The IC contribution was obtained for $p_{t0} = 2$ GeV as discussed in the main text. The H3a parametrization of the cosmic ray flux is used in this calculation. The shaded band represents the results from Ref. [3] for the astrophysical neutrino flux.

contributions. The predictions were obtained considering different models for the uPDFs and distinct values for P_{ic} in the calculation of the prompt contribution. Moreover, for the conventional atmospheric neutrino flux we assume the result derived in Ref. [32]. The resulting predictions are compared with the IceCube data obtained in Ref. [2] for the zenith-averaged flux of atmospheric neutrinos. For completeness, the results from Ref. [3] for the astrophysical neutrino flux are represented by the grey band. One has that the prompt contribution enhances the flux at large neutrino energies, with the enhancement being strongly dependent on the magnitude of the $cg \rightarrow cg$ mechanism and the uPDF considered as input in the calculations. If this mechanism is disregarded, the results represented by “Conv. + gg” in the figures indicate that the impact of the prompt flux is small in the current kinematical range probed by IceCube. In particular, it is negligible when the saturation effects are taken into account [see Fig. 8 (b)]. On the other hand, the inclusion of the $cg \rightarrow cg$ mechanism implies a large enhancement of the prompt flux at large E_ν , with the associated magnitude being strongly dependent on the value of P_{ic} . Our results for the KMR uPDF, presented in Fig. 8 (a), indicate that a value of P_{ic} larger than 1.5% implies a prediction for neutrino flux that overestimate the IceCube data at high energies. We have verified that a similar result is obtained for the KS linear uPDF (not shown explicitly). Therefore, the results derived assuming that the QCD dynamics is described by linear evolution equations, which disregard the saturation effects, indicate that in order to describe the current IceCube data we should have $P_{ic} \lesssim 1.5\%$. Surely, future data can be more restrictive in the acceptable range of values for P_{ic} . In contrast, the results presented in Fig. 8 (b) suggest the presence of saturation effects with $P_{ic} = 1.5\%$ is not discarded by the current IceCube data. It is important to emphasize that the values of the P_{ic} probabilities suggested above could be slightly decreased if a smaller value of the p_{t0} parameter was used in the numerical calculations of the $cg^* \rightarrow cg$ cross section.

However, from these results we can conclude that currently we have two acceptable so-

lutions when the $cg \rightarrow cg$ mechanism is included in the analysis: (a) the QCD dynamics is described by a linear evolution equation and the amount of IC in the proton wave function is similar to that predicted by the CT14nnloIC parameterization; or (b) the amount of IC is larger than that described by the CT14nnloIC parameterization and the saturation effects are needed to describe the charm production at very forward rapidities. One has that if the amount of IC is constrained in hadronic colliders, the IceCube data for the atmospheric neutrino flux can be considered as a probe of the QCD dynamics at high energies. Inversely, if the saturation effects are probed in hadronic colliders, the IceCube data can be used to constrain the amount of the IC. Such results demonstrate synergy between IceCube and the LHC, and strongly motivate new experimental and theoretical analyses in the future.

IV. SUMMARY

One of the main goals of the IceCube observatory is the study of astrophysical neutrinos. In order to separate the associated component, it is fundamental to have theoretical control of the background related to the atmospheric neutrino flux, where the neutrinos are generated from the decay of particles produced in high energy interactions between the Cosmic Rays and the atmosphere. In particular, the contribution of the prompt neutrino flux is still a theme of intense debate, since its magnitude for the IceCube Observatory and future neutrino telescopes depends on our knowledge about the QCD dynamics at high energies and on the large- x $c\bar{c}$ partonic content of hadrons. In this paper, we have investigated the impact of the intrinsic charm component in the hadron wave function, which carries a large fraction of the hadron momentum, and from saturation effects, associated with nonlinear corrections in the QCD evolution, in the prompt neutrino flux. Our results has indicated that the inclusion of the $cg \rightarrow cg$ mechanism has a strong effect on the prompt neutrino flux. In particular, when the IC component is present, such a mechanism determines the energy dependence of the flux at high energies, with the normalization dependent on the value assumed for the probability to find the IC in the proton wave function. Furthermore, we find that the saturation effects suppress the prompt flux in the kinematical range probed by the IceCube. The comparison of our predictions with the current IceCube experimental data has indicated that for a linear QCD dynamics, P_{ic} can be of the order of the value assumed by the CT14nnlo parametrization. In contrast, a somewhat larger value is still acceptable when a nonlinear QCD dynamics is included. Consequently, in order to disentangle these two possibilities, it is mandatory to have a better theoretical and experimental control of the prompt neutrino flux at IceCube and of the charm production at the LHC. Such a result strongly motivates the analysis of other processes that allow us to probe the presence of the intrinsic charm and constrain the description of the QCD dynamics at high energies. One of such alternatives is the analysis of the D -meson and ν_μ neutrino production at FASER [54] taking into account both effects, which we intend to study in a forthcoming publication.

ACKNOWLEDGMENTS

VPG was partially financed by the Brazilian funding agencies CNPq, FAPERGS and INCT-FNA (process number 464898/2014-5). components in mesons. This study was also partially supported by the Polish National Science Center grant UMO-2018/31/B/ST2/03537 and by the Center for Innovation and Transfer of Natural Sciences and Engineering Knowl-

-
- [1] P. A. Zyla *et al.* [Particle Data Group], PTEP **2020**, no.8, 083C01 (2020).
 - [2] M. G. Aartsen *et al.* [IceCube], Eur. Phys. J. C **75**, no.3, 116 (2015).
 - [3] M. G. Aartsen *et al.* [IceCube Collaboration], Astrophys. J. **833**, 3 (2016).
 - [4] M. G. Aartsen *et al.* [IceCube], Eur. Phys. J. C **77**, no.10, 692 (2017).
 - [5] R. Aaij *et al.* [LHCb], Nucl. Phys. B **871**, 1-20 (2013).
 - [6] R. Aaij *et al.* [LHCb], JHEP **03**, 159 (2016) [erratum: JHEP **09**, 013 (2016); erratum: JHEP **05**, 074 (2017).]
 - [7] S. Acharya *et al.* [ALICE], Eur. Phys. J. C **77**, no.8, 550 (2017).
 - [8] S. Acharya *et al.* [ALICE], Eur. Phys. J. C **79**, no.5, 388 (2019).
 - [9] V. P. Goncalves, R. Maciula, R. Pasechnik and A. Szczurek, Phys. Rev. D **96**, no.9, 094026 (2017).
 - [10] M. Ahlers, K. Helbing and C. Pérez de los Heros, Eur. Phys. J. C **78**, no.11, 924 (2018); M. Ahlers and F. Halzen, Prog. Part. Nucl. Phys. **102**, 73-88 (2018).
 - [11] M. V. Garzelli, S. Moch and G. Sigl, JHEP **1510**, 115 (2015).
 - [12] A. Bhattacharya, R. Enberg, M. H. Reno, I. Sarcevic and A. Stasto, JHEP **1506**, 110 (2015).
 - [13] R. Gauld, J. Rojo, L. Rottoli and J. Talbert, JHEP **1511**, 009 (2015); R. Gauld, J. Rojo, L. Rottoli, S. Sarkar and J. Talbert, JHEP **1602**, 130 (2016).
 - [14] F. Halzen and L. Wille, Phys. Rev. D **94**, 014014 (2016).
 - [15] A. Bhattacharya, R. Enberg, Y. S. Jeong, C. S. Kim, M. H. Reno, I. Sarcevic and A. Stasto, JHEP **1611**, 167 (2016).
 - [16] R. Laha and S. J. Brodsky, Phys. Rev. D **96**, 123002 (2017).
 - [17] M. V. Garzelli *et al.* [PROSA Collaboration], JHEP **1705**, 004 (2017); M. Benzke, M. V. Garzelli, B. Kniehl, G. Kramer, S. Moch and G. Sigl, JHEP **1712**, 021 (2017); O. Zenaiev *et al.* [PROSA], JHEP **04**, 118 (2020).
 - [18] A. V. Giannini, V. P. Goncalves and F. S. Navarra, Phys. Rev. D **98**, no. 1, 014012 (2018).
 - [19] V. P. Goncalves, R. Maciula and A. Szczurek, Phys. Lett. B **794**, 29-35 (2019).
 - [20] S. J. Brodsky, P. Hoyer, C. Peterson and N. Sakai, Phys. Lett. B **93**, 451 (1980).
 - [21] S. Paiva, M. Nielsen, F. S. Navarra, F. O. Duraes and L. L. Barz, Mod. Phys. Lett. A **13**, 2715 (1998); F. S. Navarra, M. Nielsen, C. A. A. Nunes and M. Teixeira, Phys. Rev. D **54**, 842 (1996).
 - [22] F. M. Steffens, W. Melnitchouk and A. W. Thomas, Eur. Phys. J. C **11**, 673 (1999).
 - [23] N. N. Nikolaev and W. Schafer, Phys. Rev. D **71**, 014023 (2005).
 - [24] H. Fujii, F. Gelis and R. Venugopalan, Phys. Rev. Lett. **95**, 162002 (2005).
 - [25] F. Dominguez, B. W. Xiao and F. Yuan, Phys. Rev. Lett. **106**, 022301 (2011).
 - [26] P. Kotko, K. Kutak, C. Marquet, E. Petreska, S. Sapeta and A. van Hameren, JHEP **09**, 106 (2015).
 - [27] F. Gelis, E. Iancu, J. Jalilian-Marian and R. Venugopalan, Ann. Rev. Nucl. Part. Sci. **60**, 463 (2010); E. Iancu and R. Venugopalan, arXiv:hep-ph/0303204; H. Weigert, Prog. Part. Nucl. Phys. **55**, 461 (2005); J. Jalilian-Marian and Y. V. Kovchegov, Prog. Part. Nucl. Phys. **56**, 104 (2006); J. L. Albacete and C. Marquet, Prog. Part. Nucl. Phys. **76**, 1 (2014).
 - [28] R. Maciula and A. Szczurek, Phys. Rev. D **97**, no.7, 074001 (2018).
 - [29] R. Maciula and A. Szczurek, JHEP **10**, 135 (2020).

- [30] P. Gondolo, G. Ingelman and M. Thunman, *Astropart. Phys.* **5**, 309 (1996).
- [31] E. V. Bugaev, A. Misaki, V. A. Naumov, T. S. Sinegovskaya, S. I. Sinegovsky and N. Takahashi, *Phys. Rev. D* **58**, 054001 (1998)
- [32] M. Honda, T. Kajita, K. Kasahara, S. Midorikawa and T. Sanuki, *Phys. Rev. D* **75**, 043006 (2007).
- [33] S. Ostapchenko, *Phys. Rev. D* **74**, no. 1, 014026 (2006).
- [34] A. V. Giannini and V. P. Gonçalves, *Eur. Phys. J. C* **79**, no.2, 158 (2019).
- [35] S. J. Brodsky, G. I. Lykasov, A. V. Lipatov and J. Smiesko, *Prog. Part. Nucl. Phys.* **114**, 103802 (2020).
- [36] R. D. Ball *et al.* [NNPDF], *Eur. Phys. J. C* **76**, no.11, 647 (2016).
- [37] T. J. Hou, S. Dulat, J. Gao, M. Guzzi, J. Huston, P. Nadolsky, C. Schmidt, J. Winter, K. Xie and C. P. Yuan, *JHEP* **02**, 059 (2018).
- [38] P. Jimenez-Delgado, T. J. Hobbs, J. T. Londergan and W. Melnitchouk, *Phys. Rev. Lett.* **116**, 019102 (2016).
- [39] S. J. Brodsky and S. Gardner, *Phys. Rev. Lett.* **116**, 019101 (2016).
- [40] I. Balitsky, *Nucl. Phys. B* **463**, 99-160 (1996); Y. V. Kovchegov, *Phys. Rev. D* **60**, 034008 (1999).
- [41] G. Watt, A. D. Martin and M. G. Ryskin, *Eur. Phys. J. C* **31**, 73-89 (2003).
- [42] R. Maciula and A. Szczurek, *Phys. Rev. D* **87**, no.9, 094022 (2013).
- [43] R. Maciula and A. Szczurek, *Phys. Rev. D* **100**, no.5, 054001 (2019).
- [44] R. Maciula and A. Szczurek, *Phys. Rev. D* **94**, no.11, 114037 (2016).
- [45] K. Kutak and S. Sapeta, *Phys. Rev. D* **86**, 094043 (2012).
- [46] K. Kutak and A. M. Stasto, *Eur. Phys. J. C* **41**, 343-351 (2005).
- [47] R. Maciula and A. Szczurek, *J. Phys. G: Nucl. Part. Phys.* **47**, 035001 (2020).
- [48] C. Peterson, D. Schlatter, I. Schmitt and P. M. Zerwas, *Phys. Rev. D* **27**, 105 (1983).
- [49] T. K. Gaisser, *Astropart. Phys.* **35**, 801 (2012).
- [50] R. Ammar, R. C. Ball, S. Banerjee, P. C. Bhat, P. Bosetti, C. Bromberg, G. E. Canough, T. Coffin, T. O. Dershem and R. L. Dixon, *et al.* *Phys. Rev. Lett.* **61**, 2185-2188 (1988)
- [51] R. Maciula and A. Szczurek, [arXiv:2105.09370 [hep-ph]].
- [52] M. G. Aartsen *et al.* [IceCube], [arXiv:1907.11699 [astro-ph.HE]].
- [53] M. G. Aartsen *et al.* [IceCube Gen2], [arXiv:2008.04323 [astro-ph.HE]].
- [54] J. L. Feng, I. Galon, F. Kling and S. Trojanowski, *Phys. Rev. D* **97**, no.3, 035001 (2018).